



---

## A NOVEL ENERGY STORAGE SYSTEM USAGE BASED ON ULTRA-CAPACITOR IN VARIABLE SPEED WIND TURBINES (VSWT) FOR POWER IMPROVEMENT

Mohsen Atash Ab-Parvar<sup>1</sup>, Hamed Hekmati<sup>2</sup>, Alireza Siadatan<sup>3,4</sup>, Mehdi Bigdeli<sup>5</sup>, Arsalan Hekmati<sup>6\*</sup>, Mehdi Bagheri<sup>7</sup>

1- Electrical Power & Energy Affairs, Islamic Republic of Iran Broadcasting (I.R.I.B), Tehran, Iran

2- Department of Electrical Engineering, University of Zanjan, Zanjan, Iran

3- Energy Systems Group, Faculty of Applied Science and Engineering, University of Toronto, Ontario, Canada

4- Department of Electrical Engineering, College of Engineering, West Tehran Branch, Islamic Azad University, Tehran, Iran

5- Department of Electrical Engineering, Zanjan Branch, Islamic Azad University, Zanjan, Iran

6- Electric Machines Research Group, Niroo Research Institute, NRI, Tehran, Iran

7- Department of Electrical and Electronic Engineering, Nazarbayev University, Astana, Kazakhstan

\*Corresponding author, [Ahekmati@nri.ac.ir](mailto:Ahekmati@nri.ac.ir)

### Abstract

Wind power as a renewable energy has the potential to become a clean energy source in almost all countries of the world but, there are lots of technical challenges that need to be addressed in advance. Wind speed variation (WSV) is one of the most important issues. Separate from its mechanical effects on wind turbines (WTs), it causes electrical power variations on WT as well. Doubly Fed Induction Generators (DFIGs) and Maximum Power Point Tracking (MPPT) system have been helpful so far but some problems such as inertia still needed to be solved. Inertia in the WTs causes a delay on MPPT.

This paper proposes a novel method to increase WTs output power in which a DFIG equipped with an energy storage system such as Ultra-capacitor helps MPPT system to track the wind variations rapidly by absorption or injection energy during the wind changes. The ultra-capacitor and control system are modeled and simulated in Matlab/Simulink® environment. The simulation results proofs that the proposed system can improve electrical power and increase electrical energy during WSVs. The simulation model will lead to more penetration of wind power and also enables engineers to optimize the system.

Index Terms - Doubly Fed Induction Generator (DFIG), Energy Storage, Power Improvement, Ultra-capacitor, Variable Speed Wind Turbines (VSWT).

**Keywords:** Energy, Storage, Capacitor, Wind Turbine

---

## 1. INTRODUCTION

### A. Previous strategies for increasing WTs electrical power.

Knowledge of environmental pollution has caused huge desire to use clean energy [1] and Wind power has been considered as the main choice for production of clean electricity in many countries during the last decade [2]. Wind power has its effects when connected to a power system due to the nature of the wind and power electronic devices [3]. Separate from the blade

aerodynamic shape, a great deal of efforts has been done to increase wind power so far such as [4] which presents a solution to increase the efficiency of WTs with a MPPT system in VSWTs. The [5] suggests a short term prediction system and [6] suggests a network power injection into the WT. The [7] suggests usage of lighter moving parts in WTs. The [8] tries to put up the WT at the optimum power point of operation, by connecting a fly wheel to the WT.

The angular velocity ( $\omega$ ) of WT shaft is proportional to wind speed. However, due to the inertia of the WT,

the rotational speed of rotor is slightly behind its optimal value during *WSP* which causes captured power reduction. In a *WT* if we use an energy storage system to compensate mechanical system inertia, it can track *WSP* more precisely and as a result the output power will increase.

### B. System description

This paper presents a novel system which increases electrical output power of a *VSWT* with ultra-capacitors equipped *DFIG* connected to grid during *WSP*s. After producing the system configuration modeling and simulation in the Simulink-Matlab®, the results are presented. It is demonstrated that ultra-capacitors can be used to increase electrical power.

The *VSWTs* with *DFIG* are becoming the most commercial and common type of wind energy source in the electricity markets of the world. Due to low power electronic converter rate and ability to supply power at constant voltage and frequency while the rotor speed varies [9], [10], [11], although the stand-alone operation of *DFIGs* is still feasible but the number of on-grid *DFIGs* are increasing in comparison with the other types of *WTs* [12]. One of the most important advantages of the *VSWT* as compared with conventional constant speed systems is the increase of wind power capture [7][9].

### C. Lithium-ion Ultra-capacitor (LIUC)

Ultra-capacitors have been used in the wind power industry for many purposes so far. The [13] and [14] have presented a model and simulation of Ultra-capacitor. In [15] and [16] Ultra-capacitor has been used to improve power quality and harmonics elimination. In [17] it has been used for voltage sag compensation. In [18] and [19] ultra-capacitors are used for elimination of power oscillations and reduction of restrictions on active and reactive power in *WT* controllers. But here we suggest using ultra-capacitor to increase electrical power of *VSWTs*.

### D. Objectives

In order to analyze the suggested Ultra-capacitor Energy Storage System (*UCES*) associated with *VSWT* and *DFIG*, it is developed and the overall topology simulated in (Fig.1). In this system, the *WSP*s are detected by an observer and the appropriate control command is sent to different relevant parts. The ultra-capacitor, as an energy storage device, stores the surplus stator energy of the *DFIG* and injects it into the DC-Link when the rotor of *WT* needs to speed up because of the wind acceleration.

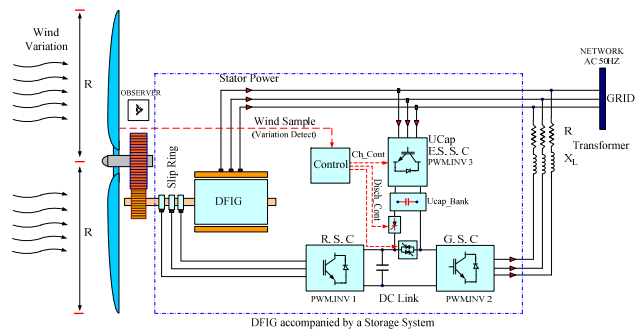


Fig. 1. VSWT WITH A DFIG ASSOCIATED WITH UCES FOR VARIABLE SPEED WIND ENERGY STORAGE

## 2. MODELING

### 2.1 Model of the Turbine

The wind power which enters the *WT* can be calculated by (1) as [20]:

$$P_{Wind} = 0.5 \rho \cdot A \cdot V_{Wind}^3 \quad (1)$$

Where  $\rho$  is the air density,  $A$  is the swept area of *WT* blade and  $V_{wind}$  is the wind speed.

The mechanical output power of a *WT* which is a nonlinear system is determined by (2) as [20]:

$$P_m = 0.5 C_p(\lambda, \beta) \cdot \rho \cdot A \cdot V_{Wind}^3 \quad (2)$$

Where  $C_p$  is the *WT* power coefficient and represents the *WT* conversion efficiency. The value of  $C_p$  can be parametrically defined by (3) and (4) as [21]. The parameters values are given in (table1).

$$C_p(\lambda_i, \beta) = C_1 \left( \frac{C_2}{\lambda_i} - C_3 \beta - C_4 \right) e^{-\frac{C_5}{\lambda_i}} + C_6 \lambda_i \quad (3)$$

$$\frac{1}{\lambda_i} = \left( \frac{1}{(\lambda_i + 0.08\beta)} - \frac{0.035}{(\beta^3 + 1)} \right) \quad (4)$$

TABLE 1. POWER COEFFICIENT ( $C_p$ ) PARAMETERS

$C_1=0.5176$	$C_2=116$	$C_3=0.4$
$C_4=5$	$C_5=21$	$C_6=0.0068$

The  $C_p$  is the function of Tip Speed Ratio (*TSR*  $\lambda$ ) and the Pitch angle ( $\beta$ ) of the blade, in a pitch controlled *WT*. The *TSR* is the speed at the tip of the *WT* blades (*Rad/s*) to the speed of wind (*m/s*). It can be defined by (5) as [20]:

$$\lambda = \frac{\omega_r \cdot R}{V_{wind}} \quad (5)$$

The *MPPT* system always tries to get the *TSR* optimum value ( $\lambda_{opt}$ ) which can be obtained from equation (6). It calculates the  $\lambda_{opt}$  value that maximizes the power coefficient. Based on the wind speed, the corresponding optimal generator speed command for maximum wind power extraction is achieved by the optimum rotor angular speed  $\omega_{r\_opt}$ .

$$\lambda_{opt} = \frac{\omega_{r\_opt} \cdot R}{V_{wind}} \quad (6)$$

Where: the  $\omega_{r\_opt}$  is the optimal angular speed of the *WT* rotor,  $R$  is the *WT* blade radius.

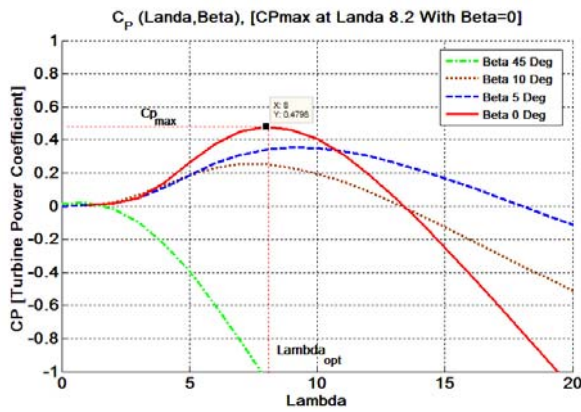


Fig. 2. AERODYNAMIC POWER COEFFICIENT ( $C_p$ ) VARIATION IN RELATION WITH  $\lambda$

By (Fig.2), it becomes clear that  $C_{p\_max}$  occurs at  $\omega_{r\_opt}$ . In fact with a *MPPT* system, the rotor of *VSWT* is controlled in such a way to obtain a pre-defined power-speed characteristic and get the optimum *AV* for every wind speed, which causes more energy extraction from the wind. But due to *WT* inertia, usually there is a delay between the *WSVs* and the rotor angular speed which causes output power reduction. By an energy storage system it becomes possible to eliminate the inertia and time delay. Since the *LIUC* has been used as an energy storage device, it is explained first.

## 2.2. LIUC Model

This paper uses a simplified equivalent *LIUC* Circuit model [13], [16] which is selected from three groups of models such as physical model [22],[23] Which is based on physical and electrochemical behavior of the Ultra-capacitors, the neural network model [24], and the equivalent circuit models [25],[26] built from series and parallel *RC* circuits whose combination results an accurate voltage current behavior on the terminals of an ultra-capacitor in the condition of charging or discharging. The terminal voltage of ultra-capacitors

can vary between values 3.8V to 2.2V during charging/discharging process (table 2) [13]. The Ultra-capacitor model is shown in (Fig.3) which includes the most important parameters. The parameters values of this model are given in (table 3). It was observed that *LIUC* capacitance is nonlinear and dependent on the open circuit voltage which is approximated by the 4th order polynomial (7) with coefficients which are listed in the (table 4) [16]. Due to very low self-discharge, it is accepted to neglect it but in the simulation, it has been modeled by  $R_p$ . More experimental tests has been done in [13]. The *LIUC* as an energy storage device has 10-20(Wh/Kg) energy density, while its power density is between 900-9000 (W/Kg) [13].

TABLE 2. ELECTRICAL PROPERTIES OF THE LIUCS[13]

Property	Nominal	Limits
Voltage (V)	3	3.8
Current (A)	10-70	200
Low Voltage Cutoff (V)	2.4	2.2

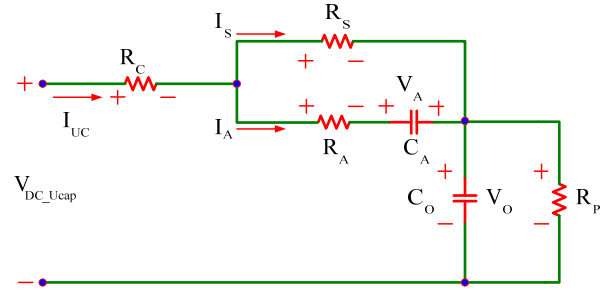


Fig. 3. LIUC EQUIVALENT CIRCUIT MODEL [13],[16]

TABLE 3. LIUC MODEL PARAMETERS [16]

$R_a$ [m $\Omega$ ]	$R_s$ [m $\Omega$ ]	$C_a$ [F]
[79.9]	[5.34]	[30.6F]

$$C_o = a.V_{oc}^4 + b.V_{oc}^3 + c.V_{oc}^2 + d.V_{oc}^1 + e \quad (7)$$

TABLE 4. THE LIUC EQUATION COEFFICIENTS[16]

a	B	C	d	E
-703.394	9359.727	45480.909	96048.083	73516.729

The equations (8-14) can be achieved by applying *KCL* and *KVL* in *LIUC* equivalent circuit model as [16]:

$$KCL : I_{sc} = I_a + I_s \quad (8)$$

$$KVL_1 : V_{dc\_Ucap} + R_c \cdot I_{sc} + R_s \cdot I_s + V_{co} = 0 \quad (9)$$

$$KVL_2 : R_s \cdot I_s - R_a \cdot I_a - V_{ca} = 0 \quad (10)$$

$$I_a = C_a \frac{dV_{ca}}{dt} \quad (11)$$

$$I_{sc} = C_o \frac{dV_{co}}{dt} \quad (12)$$

$$\begin{bmatrix} \frac{dV_{C_o}}{dt} \\ \frac{dV_{C_c}}{dt} \end{bmatrix} = \begin{bmatrix} 0 & 0 \\ 0 & -\frac{1}{C_a \cdot (R_s + R_a)} \end{bmatrix} \begin{bmatrix} V_{C_o} \\ V_{C_c} \end{bmatrix} + \begin{bmatrix} \frac{1}{C_o} \\ \frac{R_a}{C_a \cdot (R_s + R_a)} \end{bmatrix} \cdot [i_{sc}] \quad (13)$$

$$V_{DC\_Ucap} = \begin{bmatrix} 1 & \frac{R_s}{(R_s + R_a)} \\ \frac{R_s}{(R_s + R_a)} & \frac{R_s \cdot R_a}{(R_s + R_a)} \end{bmatrix} \begin{bmatrix} V_{C_o} \\ V_{C_c} \end{bmatrix} + \begin{bmatrix} R_c \\ \frac{R_s \cdot R_a}{(R_s + R_a)} \end{bmatrix} \cdot [i_{sc}] \quad (14)$$

The energy of the LIUC can vary between a maximum and minimum value and it is achieved by (15).

$$\Delta E_{UC} = 0.5 C_{UC} (u_{Uc\_dmax}^2 - u_{Uc\_dmin}^2) \quad (15)$$

Although the stored energy in an ultra-capacitor is more than a conventional capacitor, but it still inadequate for changing AV of a turbine with high inertia. By forming an ultra-capacitor bank (UCB), enough energy could be achieved. In order to inject the stored energy of the UCB into the rotor, it should be connected to Dc-link by its switches.

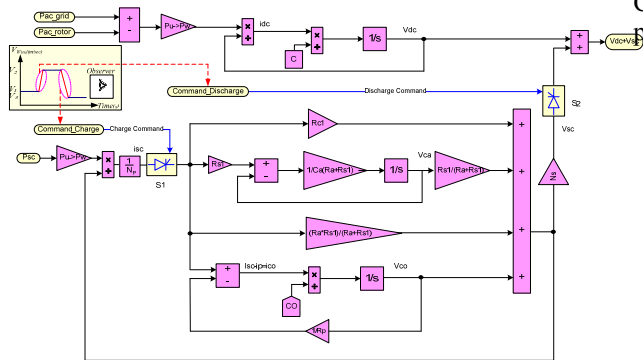


Fig. 4. THE PROPOSED LIUC BANK CONNECTED TO DC-LINK WITH SWITCHES S1&S2

Fig.4 illustrates the LIUC Bank model which is used in the simulation.  $N_s$  &  $N_p$  represent the numbers of cells (in series & parallel) and  $S_1$  &  $S_2$  are the Charge/discharge switches.

It is clear that the DC voltage of the LIUCB would vary between a maximum and minimum during its operation but in order to have the best results; it needs to operate near its optimum value (16). The controller is programed to avoid falling below the minimum voltage.

$$U_{Uc\_opt} = \sqrt{0.5(u_{Uc\_dmax}^2 + u_{Uc\_dmin}^2)} \quad (16)$$

To produce the Dc-link 1,250 volts by the LIUCB in the worst case, 22 cells are needed in series so we have (17).

$$N_s = \frac{1250 - u_{DC-Link}}{u_{Uc\_min}} \quad (17)$$

This number of Ultra-capacitor cells will cause maximum 1281.4 volts in the Dc-link, therefor

according to (16), the optimal value would be 1268 volts.

By injection of the ultra-capacitor bank energy into the DFIG rotor or storing surplus power of DFIG, acceleration or deceleration of a WT could be achieved.

### 2.3 The UCES System

During the WSV in a VSWT having MPPT system, the extractable power of the WT is controlled to achieve a pre-set power-speed characteristic. Because of WT inertia, usually there is a delay between the WSVs and the corresponding rotor angular speed which causes output power reduction. In order to increase the electrical output power of the WT during these changes, the UCES is used. This system stores surplus energy by absorbing the stator excess energy during the decrease of wind speed (Fig.6A) causing deceleration of the WT rotor during the time period of  $(t_3-t_4)$  (Fig.5) and on the other hand it injects sufficient stored energy into the rotor when wind speed increases (Fig.6B) causing acceleration of the WT rotor during the time period of  $(t_1-t_2)$  (Fig.5).

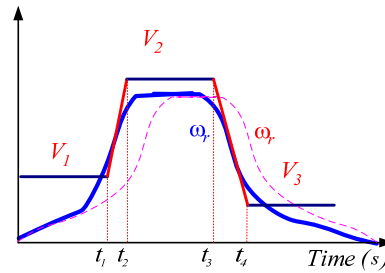


Fig. 5. SURPLUSE ELECTRICAL POWER STORAGE IN UCB DURING  $(t_3-t_4)$  AND INJECTION UCB POWER INTO DC-LINK DURING  $(t_1-t_2)$

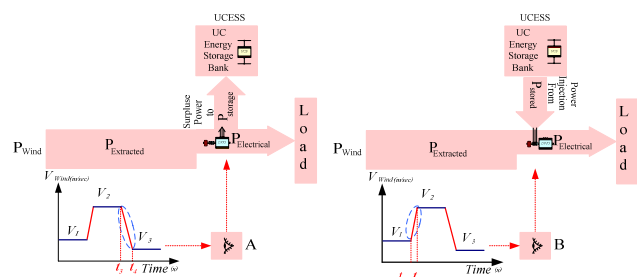
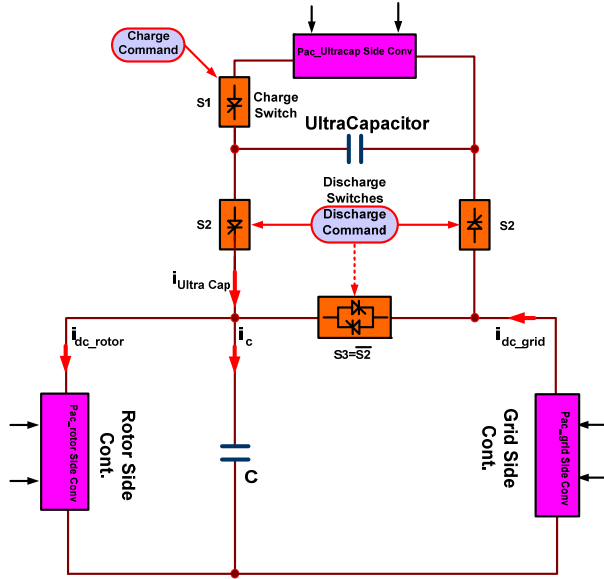


Figure. 6. UCES CONTROLLER, STORAGE /INJECTION OF ENERGY

Both of these actions are applied to overcome the inertia of the WT and would let the MPPT system to follow its target faster than before. It causes an increase of DFIG electrical output power as a result. These two functions

significantly cause the  $C_p$  Correction as well. The output signal of controller is shown in (Fig.11). *UCESS* charge/discharge simplified switching diagram is illustrated in (Fig.7). The Ultra-capacitor Converter stores stator excess power ( $P_{UC.conv}$ ) in the *UCB* during the period ( $t_3-t_4$ ), while the switches ( $S_1, S_3$ ) are closed and  $S_2$  open. During the period ( $t_1, t_2$ ) the switches  $S_2$  are closed ( $S_1, S_3$  open) causing power injection to Dc-link.



**Fig. 7. THE PROPOSED LIUC DC-LINK CONNECTION WITH ITS SWITCHES**

In order to have better performance of *UCESS*, the *UCB* should never be fully charged to  $3.8V/Cell$  or fully discharged to  $2.2 V/Cell$  otherwise it would not act perfectly correct. To meet this limitation, the stored energy in the *UCB* and the energy storage of *UCESS* should obey the equation (18).

$$\begin{aligned} \Delta E_{UCB\_Stored} &= 0.5C_{UCB}(u_{Ucb\_dcopt}^2 - u_{Ucb\_demin}^2) = \\ \Delta E_{UCB\_Storeable} &= 0.5C_{UCB}(u_{Ucb\_dcmx}^2 - u_{Ucb\_dcopt}^2) \end{aligned} \quad (18)$$

Therefore the optimum voltage would be very close to the mean value of the voltage (19).

$$u_{Ucb\_mean} \approx u_{Ucb\_dcopt} = \sqrt{0.5(u_{Ucb\_dcmx}^2 + u_{Ucb\_demin}^2)} \quad (19)$$

## 2.4. The DFIG

As it is shown in (Fig.10) Associated with a *VSWT*, an on-grid *DFIG* phasor model has been used which is the same as the wound rotor asynchronous machine with

the positive-sequence equipped with a Back to Back (*AC/DC/AC*) converter which has three main components: the Rotor-Side Converter (*RSC*), the Grid-Side Converter (*GSC*) and the Dc-link which connects these two converters. The converters are located between the rotor and the grid, have the ability to convert the electrical power to both sides. There is also a capacitor acting as a DC voltage source in the Dc-link. The three-phase stator windings are directly connected to the grid and the three-phase rotor windings are connected to *RSC* by slip rings and brushes.

The *UCESS* is added to the combination of *WT& DFIG*. This system has also an observer which receives the wind signal to analyze and detect the increase or decrease of wind speed. An additional converter, as the Ultra-capacitor Converter (*UCC*) is added and directly connected to the stator to use its surplus power to charge the *UCB* during wind signal falling time (Fig.6A). The system also helps the *WT* to speed up faster than before during wind signal raise by injection the stored energy of *UCB* into the Dc-link (Fig.6B). Although the *GSC* controls the Dc-link voltage level, but during the injection of *UCB* power into the Dc-link, the stored electrical power of Ultra-capacitors ( $P_{Ucap\_stored}$ ) effect on the Dc-link and causes DC voltage rise which could be calculated by (20).

$$V_{Dc-Link} + N_s \left[ V_{Co} + \frac{R_s}{(R_s + R_a)} V_{Ca} + R_c i_{sc} + \frac{R_s R_a}{(R_s + R_a)} i_{sc} \right] \quad (20)$$

Since the *RSC* has the ability to supply the suitable power which is needed by the rotor, the Dc-link voltage rise causes acceleration of the rotor angular speed and also a rise of *DFIG* electrical output power (Fig.19).

From the grid side point of view, to maintain the power balance, the stator, rotor and Ultra-capacitor power are algebraically added. In order to calculate the Dc-link power the equation (21) could be used, if the converter loss is neglected.

$$P_{dc} = P_{ac\_gs.Conv} + P_{ac\_rs.Conv} + P_{UC.Conv} \quad (21)$$

The  $P_{UC.Conv}$  is the injected Power by *UCB* into the Dc-link only during the wind signal rise.

## 2.5. Lithium-Ion UCES System control

The function of *UCES* control system can be summarized and explained by the presented flowchart (Fig.8). The novel proposed algorithm of *UCESS* operation causes a power increase in *VSWT* with *DFIG*. In this method a central control observes the wind signals and modifies the electrical output power of the *DFIG* which is based on energy storage/injection of a

LIUCB. It is easy to implement the system since it is a simple method.

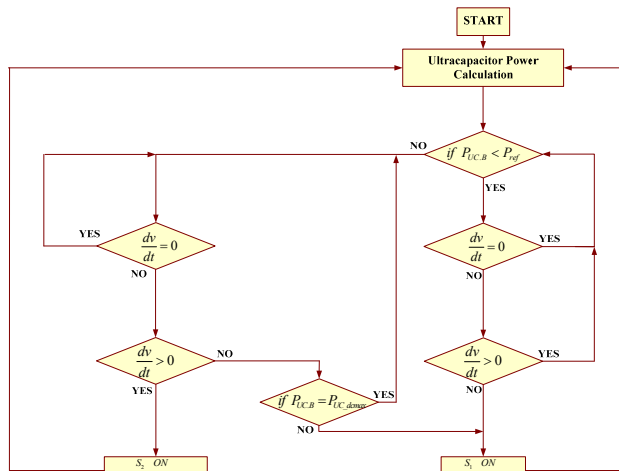


**Fig. 8. LITHIUM-ION UCES FLOWCHART (OBSERVATION & CONTROL) METHOD FOR POWER IMPROVEMENT**

### 2.6 Turbine Model

As it is mentioned in (1.4) a VSWT Associated with a DFIG phasor model for the simulation has been used which is the wound rotor asynchronous machine with the positive-sequence. This on grid turbine model is the same which is provided in Matlab-Simulink Simpower System™ library. This WT has the MPPT system and pitch control. The pitch angle is kept constant at zero degree until the wind speed reaches the point *D* of the tracking characteristics. Beyond the point *D* the pitch angle is proportional to the wind speed deviation from the *D* point. During the simulation, in the operation Control parameters menu, the Var Regulation mode Has been selected, therefor the generated reactive power has been set to be zero,  $Q_{ref}(pu)=0$

### 3. SYSTEM SIMULATION IN SIMULINK-MATLAB®

The Simulink implementation of the LIUC the model based on equations (8)-(14) is shown in (Fig.9)

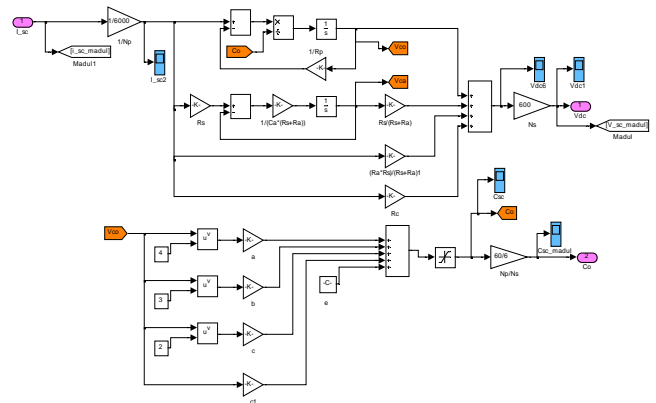


**Fig. 9. LITHIUM-ION ULTRA-CAPACITOR BANK SIMULATION**

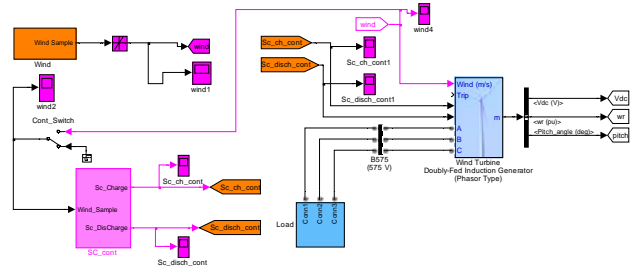


**Fig. 10. SIMULATION OF WT ON GRID CONNECTION ULTRA-CAPACITOR CONTROLLER & OBSERVER SYSTEM WITH WIND SIGNAL GENERATOR**

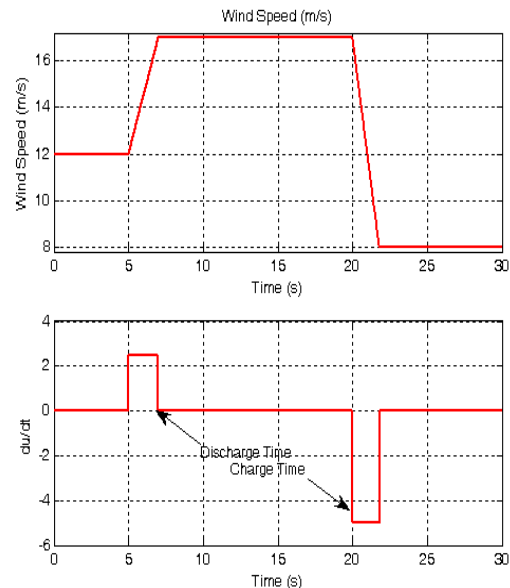


**Fig. 11. DETECTION OF WSVS FROM WIND SAMPLE**

## 4. RESULTS AND DISCUSSIONS

The wind speed sample (Fig.12) which is produced by wind signal simulator using Band-Limited White Noise is applied to the VSWT with a DFIG (Fig.10) and the results show that LIUC used in Proposed UCESB could increase the output power of the DFIG (Fig.19). The processes of charge & discharge (Fig.16, 17) of UCESB could help the MPPT system to speed up the tracking of the WSVs by acceleration of the rotor speed (Fig.14&15) and also could correct  $C_p$  (Fig.13). Connection of the UCESB to the Dc-link causes an increase of the DC voltage level form 1200 volts to even more than 1281.4 volts which (Fig. 16) is the evidence of this concept.

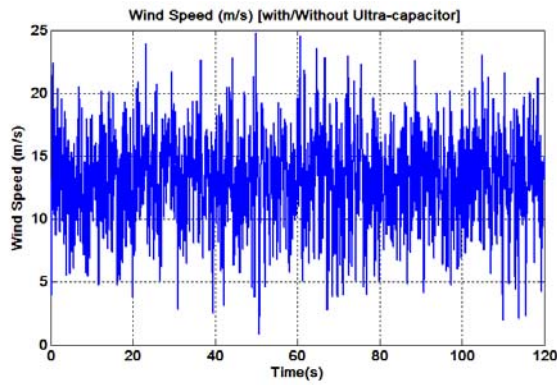


Fig. 12. APPLIED VARIABLE WIND SPEED TO VSWT DFIG ASSOCIATED WITH UCESB

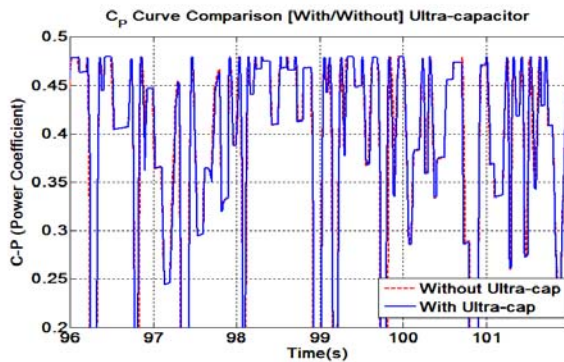


Fig. 13.  $C_p$  COMPARISON [WITH/WITHOUT] UCESB

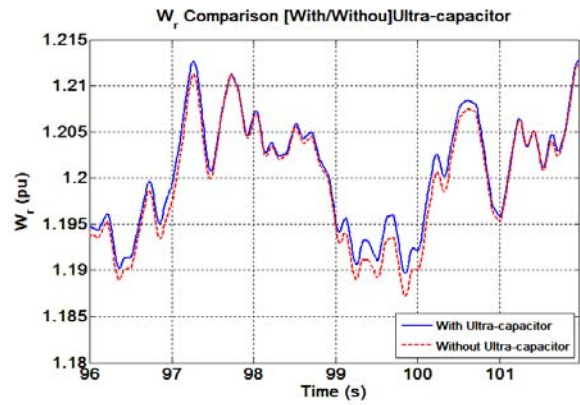


Fig. 14. MAGNIFIED  $\Omega_R$  COMPARISON [WITH/WITHOUT] UCESB

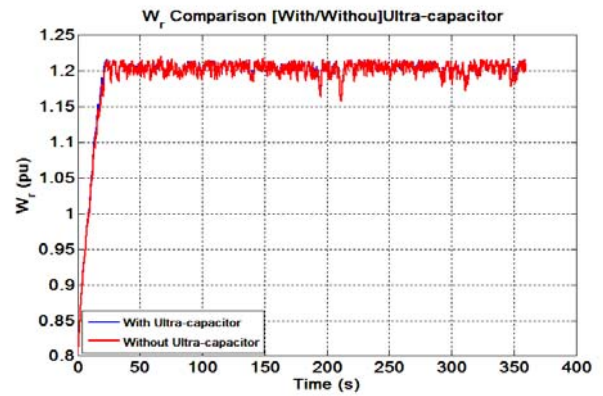


Fig. 15.  $\omega_r$  COMPARISON [WITH/WITHOUT] UCESB

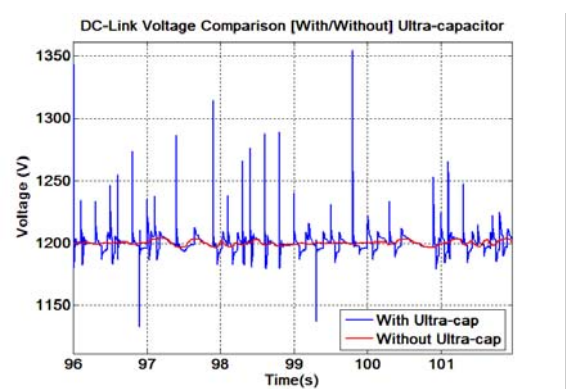


Fig. 16. MAGNIFIED DC-LINK VOLTAGE COMPARISON [WITH/WITHOUT] UCESB

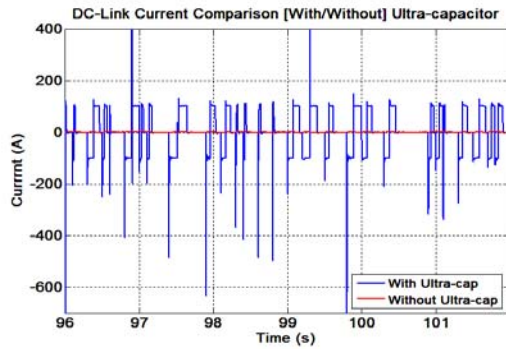


Fig. 17. MAGNIFIED CURRENT COMPARISON [WITH/WITHOUT] UCESS

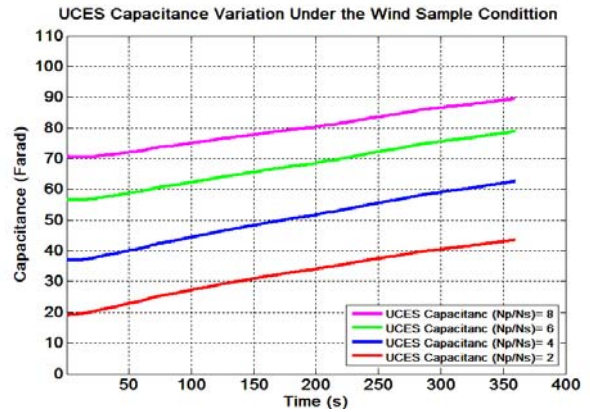


Fig. 20. UCES BANK CAPACITANCE VARIATION UNDER APPLIED WIND SAMPLE THE CONDITION

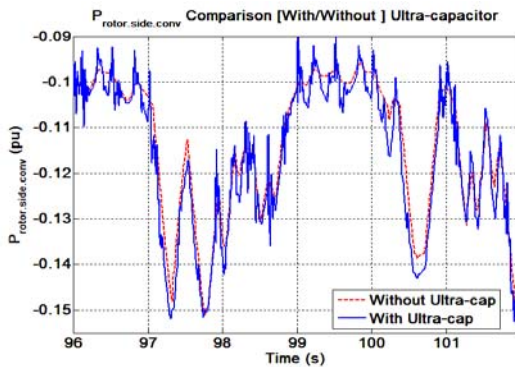


Fig. 18. MAGNIFIED ABSORB ROTOR POWER INCREASE WITH UCESS COMPARE WITH NO UCESS

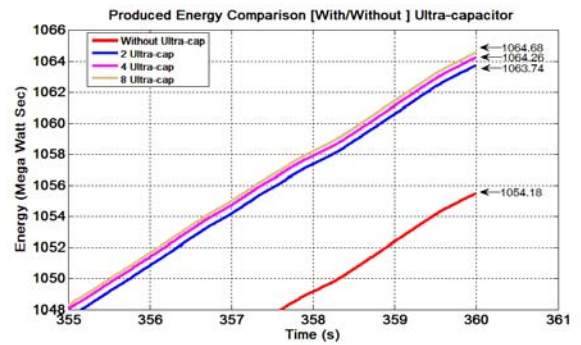


Fig. 21. DFIG ELECTRICAL ENERGY OUTPUT COMPARISON [WITH/WITHOUT UCESS] AND EFFECT OF CAPACITANCE

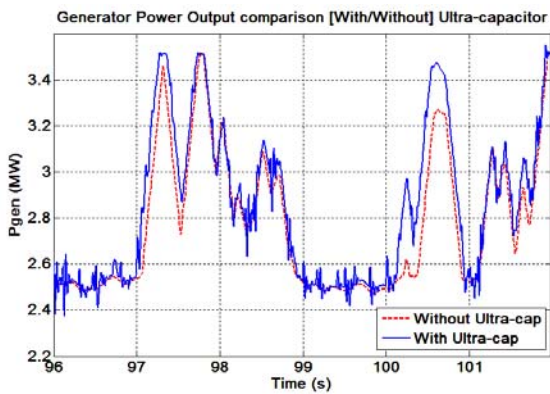


Fig.19. MAGNIFIED DFIG ELECTRICAL POWER OUTPUT INCREASE WITH UCESS UNDER APPLIED WIND SAMPLE

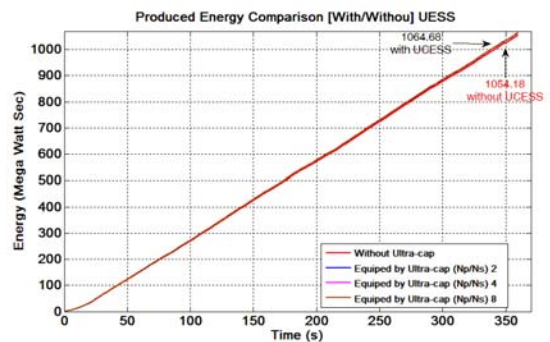


Fig. 22. DFIG ELECTRICAL ENERGY OUTPUT COMPARISON [WITH/WITHOUT] UCESS

TABLE. 5. DFIG OUTPUT ENERGY[MWH] VARIATION WITH DIFFERENT CAPACITANCE OF ULTRA-CAPACITOR

No	$N_p/N_s$ Ratio	$C_o$ (F)	$E_{UCES}$	$E_{Out}$
1	0	–	–	$\frac{1054.18 \times 10}{3600}$
2	2	19.09 – 43.35	$\frac{54.65 \times 10}{3600}$	$\frac{1062.78 \times 10}{3600}$
3	4	36.85 – 62.43	$\frac{55.11 \times 10}{3600}$	$\frac{1063.49 \times 10}{3600}$
4	6	56.55 – 78.87	$\frac{55.16 \times 10}{3600}$	$\frac{1063.80 \times 10}{3600}$
5	8	70.68 – 82.38	$\frac{55.29 \times 10}{3600}$	$\frac{1064.68 \times 10}{3600}$

TABLE. 6. DFIG OUTPUT ENERGY COMPARISON WITH UCESB [( $N_p/N_s=8$ ) & 1200-1930VDC&CO=76.755FARAD]

E (Per*)	$E_{Net}$ (MWh)	$E_{Out\_UCESB}$ (MWh)	$E_{Out\_NoUC}$ (MWh)
*Hour	0.0291	2.9574	2.9283
*Day	0.7	70.9786	70.28
*Month	21	2129.36	2108.36
*Year	255.5	25907.21	25651.71

It is also clear that the Dc-link voltage should be eliminated (for example between two values 1280-1250V) in order to avoid over voltage damages. The (Fig.17) illustrates the discharge current of LIUC in the Dc-link. To avoid side effects of this discharge current [such as:  $L(di/dt)$ ] damages it is necessary to eliminate this current (for example  $\pm 150A$ ). During the function of UCCESS the absorbed power by rotor increases (Fig.18). As it mentioned in 2.1 the capacitance of LIUC is nonlinear (Fig.20). According to the (table.5) the output power of DFIG is proportional to the ratio of LIUC capacitance [( $N_p/N_s$ ) =2, 4, 6, 8]. The higher capacity causes the higher power (Fig.20&Fig.21). Due to what conveys the (Fig.19), the DFIG electrical output power increases if the proposed system is used. The (Fig.21&Fig.22) illustrate that by VSWT and DFIG without UCCESS under the wind sample regime could produce 2.928 (MWh) while by utilization the proposed UCCESS [( $N_p/N_s$ ) =8, at 1250.6 to 1281.4 DC Volts] the output power could increase as much as 2.957(MWh). It means 1% increase in power production and if the applied wind sample still the same for 24hours a day, 30 days per month and 365 days per year, the net increased production energy annually would be 255.5 (MWh) for a 3.6MW WT (table.6) and Over production energy of six wind turbine which are equipped with proposed UCCESS during 20 years could be equal to annual

electrical energy produced by one turbine with the same power.

## 5. CONCLUSION

The new model of smart UCES system which is proposed in this paper provides more wind power penetration by increasing a DFIG output power driven by the VSWT with utilization of Lithium-ion Ultra-capacitors.

It has a substantial impact on the annual energy capture of the WT. The UCCESS control is presented and the system is tested in Simulink-Matlab to examine power increase capability and also the control algorithm of the proposed system and its strategies are described. Several capacitances configurations of LIUCs were investigated and their impacts on WT DFIG output were shown.

It has been examined that the acceleration and deceleration of WT during the wind speed changes can increase electrical output power. Due to no chemical products during charge/discharge, no memory effect and almost no loss in Ultra-capacitors make their life time benefit able. Note that technology development would help to manufacture a very high quality Ultra-capacitors in near future. Despite of the disadvantages UCES (mechanical tensions which effect on moving parts, the need of Dc-link voltage elimination); the authors proposed a novel technic by Lithium-Ion UCCESS to electrical wind power increase which will help more WTs penetration in the world. Other advantages of Ultra-capacitors are their low volume, weight and also the small installation footprint. It should be noted that due to there is no moving part in the UCCESS, their system maintenance is cheap and remember that the nature of LIUC short time energy storage in the proposed method is compatible with the nature of wind speed changes.

## 6. NOMENCLATURE

$\rho$ =Air Density(Kg/m<sup>3</sup>),  $A$ =Area(m<sup>2</sup>),  $V_{Wind}$ = Wind Speed(m/s),  $P_m$ =Mechanical Power (W),  $C_p$ =Power Coefficient,  $R_T$ =Turbine Blade Radius,  $\omega_T$ =WT Angular Velocity (AV) (rad/s),  $\omega_r$ =Rotor AV (rad/s),  $E_{uc}$ =Ultra-cap Energy,  $u_{uc}$ = Ultra-cap Vlotage (Volts),  $C_{uc}$ = Ultra-cap Capacitance(F),  $P_{uc,Conv}$ =Ultra-cap Power,  $\beta$ =Pitch Angle(dedree),  $\lambda$ =Tip Speed Ratio(TSR),  $\omega_{Opt\_ref}$ =Cont. ref. angular speed

## 7. REFERENCES

- [1] A. Hekmati, R. Hekmati, "Double pancake superconducting coil design for maximum magnetic energy storage in small scale SMES systems", *Cryogenics*, Vol 80, PP. 74–81, 2016.
- [2] H. Rezvani, A. Hekmati, "Wind Diesel Hybrid System without Battery Energy Storage Using Imperialist Competitive Algorithm", *International Journal of Electrical, Computer, Energetic, Electronic and Communication Engineering*, vol. 9, No. 6, pp. 560-565, 2015.
- [3] V. Nurmanova, M. Bagheri, A. Sultanbek, A. Hekmati, H. Bevrani, "Feasibility study on wind energy harvesting system implementation in moving trains", *International Siberian Conference on Control and Communications (SIBCON)*, 2017, Doi: 10.1109/SIBCON.2017.7998495.
- [4] A.M De Bore, S. Drouilhet and V.Gevorgian,"A peak Power Tracker for Small Wind Turbines in Battery Charging Applications," *IEEE trans. Ergy Conversion*", vol.14, no.4, PP.1630-1635, Dec.1999.
- [5] F. Salehi,"Increasing Detected Wind Energy, Using Short Time Prediction of Wind Speed and Injecting Power from Network to Wind Turbine in Time Necessary". Master's thesis, *Amirkabir University*, 2008
- [6] B. Sedaghat,"A Study of Injection Power from Network to Wind Turbine in order to send the Wind turbine Back to its Optimal Condition." *Amirkabir University*, Master Thesis, 2007.
- [7] J. Sallan, J.F sanz, A. Iombart, M.P. Comech, and J. L.Villa,"Efficiency Improvement in Wind Turbines by Increasing Speed Range Using Tandem Connection Scheme," *IEEE Int. Symposium On Industrial Electronics*, PP. 2625-2630, 2007.
- [8] A. Koyangi, H. Nakamura, Kobayashi, Y, Suzuki and R. Shimada,"study on Maximum Power Point Tracking of Wind Turbine Generator Using A Flywheel", *Proceedings of the Power IEEE, Conversion Conference, PCC Osaka*. vol.1, PP.322-327, 2002.
- [9] M.Verij Kazemi, A. S. Yazdankhah, H. M. Kojabadi, "Direct power control of DFIG based on discrete space vector modulation", *Elsevier, Renewable Energy*, Vol.35, pp.1033-1042, 2010.
- [10] R. Datta and V.T. Ranganathan,"Variable speed wind power generation using doubly fed wound rotor machine-a comparison with alternatives schemes," *IEEE trans. Energy Conversion*, vol.17, pp.414- 421, no. 3, Sept 2002
- [11] P.Pourbeik, R. J. Koessler, D. L. Dickmader and W.Wong,"Integration of large wind farms in to utility grids Part2-performance. *IEEE* vol.3, 1520-1525, July 2003.
- [12] R. Penaa, R. Cardenasb, E. Escobarb, J. Clarec, P. Wheelerc, "Control strategy for a doubly-fed induction generator feeding an unbalanced grid or stand-alone load", Elsevier, *Electric Power Systems Research*, Vol. 79, no.2, pp. 355- 364, Feb.2009.
- [13] Emad Manla, Goran Mandic and Adle Nasiri," Testing and Modeling of Lithium-Ion Ultra-capacitors" *IEEE, Energy Conversion Congress and Exposition (ECCE)*, PP. 2957-2962, Sept 2011.
- [14] Patrik Johnsson, Bjorn and Andersson," Comparison of Simulation Programs for Supercapacitor Modeling-Model Creation and Verification" Master of Science Thesis, *Chalmers University of Technology*, Gothenburg, Sweden, 2008.
- [15] Mohamad Rashed, Abd El-Hady Ghanem, Adel El-Sayes and III. Mansy, "Control Strategy for an Isolated DFIG Based Micro-Grid with Integrated Super-Capacitors", *Online Journal on Electronics and Electrical Engineering (OJEEE)*, Vol.1, no.2, PP.81-88, Ref No: W09-0015, 2009.
- [16] Gorand Mandic,"Lithium-Ion Ultra-capacitor Energy Storage Integrated with a Variable Speed Turbine for Improved Power Conversion Control," *University of Wisconsin Milwaukee Theses and Dissertations*. Paper201, 2012.
- [17] Leonardo Manuel Plma Fanjul,"Some New Applications of Super-capacitors in Power Electronics," *Texas A&M University*, Master's thesis, August 2003.
- [18] Sowmini. Priya. S, Rajakumar. S,"An Energy Storage System for Wind Turbine Generators Battery and Super-capacitor," *International Journal of Engineering Research and Applications (IJERA)*, vol.3, no.2, pp.1219-1223, March-April 2013.
- [19] M.Al -Ramadhan, M. A. Abido, "Design and Simulation of Super-capacitor Energy Storage System," *International Conference on Renewable Energies and Power Quality (ICREPO12)*, Santiago de Compostela (Spain), March 2012.
- [20] G. M. Masters, "Renewable and Efficient Electric Power Systems", *IEEE press, Wiley-Interscience*, Hoboken, New Jersey, PP.307-383, 2004.
- [21] Heier, Siegfried."Grid Integration of Wind Energy Conversion Systems; *John Wiley & Sons Ltd*. Hoboken, NJ, USA, 1998. ISBN0-471-97143-X
- [22] J. L. Rodriguez-Amenedo, S. Arnalte, and J.C. Burgos,"Automatic generation control of a wind farm with variable speed wind turbines," *IEEE Trans. Energy Convers.*, vol. 17, no.2, pp. 279-284, Jun.2002.
- [23] R. G. de Almeida and J. A. P. Lopes, "Participation of doubly fed induction wind generators in system

- frequency regulation,"*IEEE Trans. Power Systems*, vol.22, no.3, pp.944–950, Aug.2007.
- [24] E. Muljadi and H. E. Mc Kenna, "Power quality issues in a hybrid power system," *IEEE trans. Ind. Appl.*, vol.38, no.3, pp.803-809, May/Jun 2002.
- [25] C. Luo and B.-T. Ooi, "Frequency deviation of thermal power plants due to wind farms," *IEEE Trans. Energy Convers.* vol.21, no.3, pp.708–716, Sep.2006.
- [26] C. Luo, H. Banakar, B. Shen; B.-T. Ooi, "Strategies to Smooth Wind Power Fluctuations of Wind Turbine Generator," *IEEE trans. Energy Convers.*, vol.22, no.2, pp.341-349, Jun.2007.